

# IL-4 impairs wound healing potential in the skin by repressing fibronectin expression

Ana P. M. Serezani, PhD,<sup>a</sup> Gunseli Bozdogan, MD,<sup>a</sup> Sarita Sehra, PhD,<sup>a</sup> Daniel Walsh, BS,<sup>a</sup> Purna Krishnamurthy, MS,<sup>a</sup> Elizabeth A. Sierra Potchanant, PhD,<sup>a,b,c</sup> Grzegorz Nalepa, MD, PhD,<sup>a,b,c</sup> Shreevrat Goenka, PhD,<sup>a</sup> Matthew J. Turner, MD, PhD,<sup>d</sup> Dan F. Spandau, PhD,<sup>d</sup> and Mark H. Kaplan, PhD<sup>a</sup>      Indianapolis, Ind

**Background:** Atopic dermatitis (AD) is characterized by intense pruritis and is a common childhood inflammatory disease.

Many factors are known to affect AD development, including the pleiotropic cytokine IL-4. Yet little is known regarding the direct effects of IL-4 on keratinocyte function.

**Objective and Methods:** In this report RNA sequencing and functional assays were used to define the effect of the allergic environment on primary keratinocyte function and wound repair in mice.

**Results:** Acute or chronic stimulation by IL-4 modified expression of more than 1000 genes expressed in human keratinocytes that are involved in a broad spectrum of nonoverlapping functions. Among the IL-4-induced changes, repression of fibronectin critically impaired the human keratinocyte wound response. Moreover, in mouse models of spontaneous and induced AD-like lesions, there was delayed re-epithelialization. Importantly, topical treatment with fibronectin restored the epidermal repair response.

**Conclusion:** Keratinocyte gene expression is critically shaped by IL-4, altering cell fate decisions, which are likely important for the clinical manifestations and pathology of allergic skin disease. (J Allergy Clin Immunol 2016;■■■:■■■-■■■.)

**Key words:** Keratinocyte, atopic dermatitis, wound healing, IL-4, RNA sequencing, fibronectin

Atopic dermatitis (AD) is one of the most common inflammatory diseases in children and is characterized by intense pruritis (itch) and abnormal skin.<sup>1-3</sup> AD is an early indicator of subsequent atopic diseases, with roughly 60% of children with AD later having airway hyperresponsiveness.<sup>4-6</sup> The pathogenesis of AD

## Abbreviations used

AD:	Atopic dermatitis
FLG:	Filaggrin
FN1:	Fibronectin 1
HK:	Human keratinocyte
IL-4R:	IL-4 receptor
IVL:	Involucrin
LOR:	Loricrin
RNA-Seq:	RNA sequencing
STAT6:	Signal transducer and activator of transcription 6
WT:	Wild-type

involves impaired keratinocyte differentiation and diminished skin barrier function, resulting in dry (xerotic) skin, increased susceptibility to bacterial and viral infections, and augmented percutaneous exposure to environmental allergens.<sup>3,7</sup>

The T<sub>H</sub>2-type cytokine IL-4 has been shown to affect keratinocyte differentiation.<sup>7,9</sup> IL-4 is a pleiotropic cytokine secreted by activated T lymphocytes and innate immune cells acting through a receptor on hematopoietic cells composed of the IL-4 receptor (IL-4R)  $\alpha$  and  $\gamma$ c receptor (type I IL-4R).<sup>10,11</sup> Keratinocytes and other nonhematopoietic cells do not express  $\gamma$ c receptors but can respond to IL-4 through the type II IL-4R composed of IL-4R $\alpha$  and IL-13 receptor  $\alpha$ 1.<sup>12</sup> IL-4 binding to either receptor mediates the phosphorylation and dimerization of signal transducer and activator of transcription 6 (STAT6), regulating transcriptional activation of genes in target cells.<sup>9</sup> Keratinocytes exposed to IL-4 exhibit reduced expression of epidermal differentiation complex genes,<sup>13</sup> decreased expression of defensins,<sup>3</sup> altered expression of keratins,<sup>14</sup> and increased production of the chemokine CCL26 (eotaxin 3).<sup>15</sup>

IL-4 is an important target in patients, and in clinical trials of subjects with moderate-to-severe AD, disease scores improved after anti-IL-4R $\alpha$  human antagonist antibody treatment.<sup>16</sup> However, there is still little known regarding the consequences of IL-4 signaling on keratinocyte differentiation and barrier protection. The current study defines the global changes induced by IL-4 on gene expression in human keratinocytes (HKs) through bioinformatics analysis of gene expression after high-throughput analysis (RNA sequencing [RNA-Seq]). This analysis identified a wound-healing pathway, including expression of fibronectin by keratinocytes, which is repressed by IL-4 treatment and likely contributes to pathology in patients with AD. Moreover, modulating this pathway in an *in vivo* model improved wound repair.

## METHODS

### Mice

Female BALB/C and C57BL/6 mice were purchased from Harlan Bioscience (Indianapolis, Ind). The generation of Stat6VT transgenic mice

From <sup>a</sup>the Department of Pediatrics, H.B. Wells Center for Pediatric Research and Department of Microbiology and Immunology; <sup>b</sup>the Division of Pediatric Hematology-Oncology Bone Marrow Failure Program; <sup>c</sup>the Department of Medical and Molecular Genetics; and <sup>d</sup>the Department of Dermatology, Indiana University School of Medicine.

Supported by Public Health Service grants R01 AI095282 (to M.H.K.), R01 ES020866 (to D.F.S.), VA CDA2 CX001019 (to M.J.T.), NIH K12-Indiana Pediatric Scientist Award, and T32 (5T32H0069047-04; to G.N.). Support provided by the HB Wells Center was in part from the Riley Children's Foundation.

Disclosure of potential conflict of interest: G. Nalepa receives grant support from the National Institutes of Health (NIH). M. J. Turner receives grant support from Department of Veterans Affairs (VA career development award CX001019). D. F. Spandau receives grant support from the NIH. M. H. Kaplan receives grant support from the National Institutes of Health. The rest of the authors declare that they have no relevant conflicts of interest.

Received for publication October 23, 2015; revised May 27, 2016; accepted for publication July 5, 2016.

Corresponding author: Mark H. Kaplan, PhD, Indiana University, Pediatrics, Wells Center, 1044 West Walnut St, Rm 202, Indianapolis, IN 46202. E-mail: [mkaplan2@iupui.edu](mailto:mkaplan2@iupui.edu). 0091-6749/\$36.00

© 2016 American Academy of Allergy, Asthma & Immunology  
<http://dx.doi.org/10.1016/j.jaci.2016.07.012>

was previously described.<sup>17</sup> These mice express the human *STAT6* gene with V547 and T548 mutated to alanine under transcriptional control of the CD2 locus control region. IL-4-deficient mice (*Il4<sup>-/-</sup>*) were purchased from the Jackson Laboratory (Bar Harbor, Me) and mated to Stat6VT transgenic mice. *Stat6<sup>-/-</sup>* mice were generated and backcrossed for at least 10 generations to BALB/c mice, as described previously.<sup>18</sup> Mouse ears were punched with a 2-mm punch (Kent Scientific, Torrington, Conn) to determine the *in vivo* wound-healing response. In some experiments mice were treated for 2 days with ointment containing BSA (Promega, Madison, Wis) or fibronectin purified from human plasma (Sigma, St Louis, Mo). Wild-type (WT) and *Stat6<sup>-/-</sup>* mice were treated with the vitamin D analogue MC903 (Calcipotriol, Sigma), as previously described, to determine the wound response in an induced model of AD-like disease.<sup>19</sup> MC903 was dissolved in 100% ethanol and topically applied on mouse ears (2 nmol in 25 µL per ear) for 5 days. Ethanol alone was used as a vehicle control. Ears were punched at day 6 after treatment. Mice were maintained in pathogen-free conditions, and all studies were approved by the Animal Care and Use Committee of the Indiana University School of Medicine.

### Keratinocyte cell culture

Primary HKs were isolated from excised foreskin tissue, as previously described,<sup>20</sup> and washed with antibiotics. The tissue was minced, and the individual cells were released from the tissue by using trypsin digestion. Keratinocytes and fibroblasts were separated by means of differential resistance to treatment with EDTA. Isolated cells were grown in EpiLife Complete Medium (Life Technologies, Grand Island, NY) with HK growth supplement (Life Technologies) and 1000 U of penicillin-streptomycin (Roche, Mannheim, Germany) and grown as unmanipulated cultures or immortalized by the expression of human telomerase reverse transcriptase.<sup>21</sup> HKs were treated with 2 mmol/L CaCl<sub>2</sub> every other day to stimulate keratinocyte differentiation. HKs were stimulated with 20 ng/mL or the indicated concentration of recombinant human IL-4 (R&D Systems, Minneapolis, Minn) or IL-13 (PeproTech, Rocky Hills, NJ). All HK samples were deidentified, and the institutional review board of the Indiana University School of Medicine certified these studies as exempt.

### Histologic and immunofluorescence analysis

Ear tissue was fixed with 10% formalin for 24 hours. Routine histologic techniques were used to paraffin embed the ears, and 5-µm sections were stained with hematoxylin and eosin or Masson trichrome. Ki-67 expression was analyzed by means of immunofluorescence with rabbit anti-human Ki-67 (SP6) antibody and anti-rabbit 488 nm. Quantitative digital morphometric analysis of the percentage of re-epithelialization was measured by using Image J 1.43u (National Institutes of Health, Bethesda, Md). The percentage of re-epithelialization was calculated by dividing the total pixel length of the lesion visualized at days 3 or 6 after wounding by the pixel length of lesions with incomplete re-epithelialization.

### In vitro wound assay and live cell imaging

Normal HKs were cultured at 100% confluence in plates covered or not with 1 µg/mL BSA (Promega) or fibronectin from human plasma (Sigma-Aldrich). HKs were cultured with calcium chloride alone in EpiLife Complete Medium and stimulated with 20 ng/mL recombinant human IL-4, as indicated. At days 2 or 5, a cell-free area was created by scratching the monolayer with a 200-µL pipette tip. Time-lapse photography was performed on an automated time-lapse imaging system (Biostation IM-Q; Nikon Instruments, Tokyo, Japan) every 2 minutes in an environmentally controlled chamber (5% CO<sub>2</sub>, 37°C, 3.2 minutes) fitted with the 20× NA 0.8 lens and a DS-Qi1 CCD camera. Photoshop (Adobe, San Jose, Calif) software platforms were used to export movies.

### Organotypic skin equivalent

*In vitro* skin equivalents were constructed by using normal primary fibroblasts and keratinocytes isolated from human neonatal foreskin, as previously

described.<sup>22</sup> Skin equivalents were grown at 35°C in an air incubator for 7 to 10 days, and fresh medium was added every 2 days.

### Cell isolation and flow cytometry

Epidermis was separated from dermis after enzymatic treatment with 400 µg/mL Liberase (Roche) for 90 minutes at 37°C. Total cells were further isolated from the epidermis by using the gentleMacs dissociator (Miltenyi Biotech, Bergisch Gladbach, Germany), according to the manufacturer's instructions. For detection of Stat6VT expression, splenocytes and total epidermal and dermal cell suspensions were preincubated with Fc-block (BD PharMingen, San Jose, Calif) for 10 minutes at 4°C before incubation with anti-CD45, anti-CD3, anti-CD4, anti-CD8, and anti-CD19 for 30 minutes at 4°C. HKs were harvested and incubated with Human TruStain FcX (BioLegend, San Diego, Calif) for 10 minutes at 4°C. The cells were fixed and permeabilized for intracellular staining with phospho-STAT6 Alexa Fluor 488 (BD PharMingen) or anti-Flag APC (DYKDDDDK tag epitope, BioLegend) antibody before analysis by means of flow cytometry (Attune Acoustic Focusing Cytometer), as previously described.<sup>23</sup> The results were analyzed with FlowJo software (Ashland, Ore).

### ELISA

CCL26 levels were measured in the supernatants of HKs by using the human Quantikine ELISA Kit (R&D Systems, Minneapolis, Minn). Fibronectin levels were measured in single-cell suspension lysates isolated from the dermis and epidermis, as described above. Fibronectin levels were measured by using a mouse ELISA kit (Abcam, Cambridge, United Kingdom), according to the manufacturer's instructions.

### Quantitative RT-PCR

Total RNA was isolated from cells and reverse transcribed, according to the manufacturer's instructions (Invitrogen Life Technologies, Carlsbad, Calif). Quantitative PCR was performed with TaqMan Fast Universal PCR Master Mix and commercially available primers (Applied Biosystems, Foster City, Calif). RNA was normalized to expression levels of β<sub>2</sub>-microglobulin, and relative expression was calculated with the 2<sup>-ΔΔCt</sup> method.

### Statistical analysis

Statistical analysis was determined by using the unpaired Student *t* test or ANOVA, followed by the Tukey test for multiple comparisons, and a *P* value of less than .05 was considered significant.

### Alignment of RNA-Seq reads to human genome

Total RNA was isolated from immortalized HKs cultured under conditions indicated above by using TRIzol reagent. RNA samples were purified with the RNase-Free DNase Kit (Qiagen, Hilden, Germany). RNA-Seq libraries were generated by Orogenetics using the HiSeq 2000 sequencing instrument with 20 million paired-end 100 nucleotide reads per sample, with biological duplicates for each condition and results displayed as average samples. The percentage of mapped reads (50% to 56% of sequences) represented 20× nucleotide coverage of the estimated transcriptome. Bioinformatics analysis was performed by the Bioinformatics Core at Indiana University School of Medicine. Short reads (fastq files) from each sample were independently aligned to human reference genome hg19 by using tophat (version 2.1.0), with default parameters and known transcriptomes. Alignment results were filtered by using bamutils v0.5.0 to remove reads with multiple mappings. Statistics data of the resulting alignment files were created with samtools (version 0.1.18) and bamutils (version 0.5.0). The counts of aligned reads mapping to known genes were calculated by using bamutils (version 0.5.0). EdgeR (version 2.11) was used for differential expression analysis. RNA-Seq data files were submitted to the Gene Expression Omnibus (accession no. GSE59275). Gene ontology analysis was performed with DAVID Bioinformatics resources.<sup>24</sup> Venn diagram analyses were generated with Venny (<http://bioinfogp.cnb.csic.es>), and heat maps were created with the MultiExperiment Viewer (<http://www.tm4.org/>).

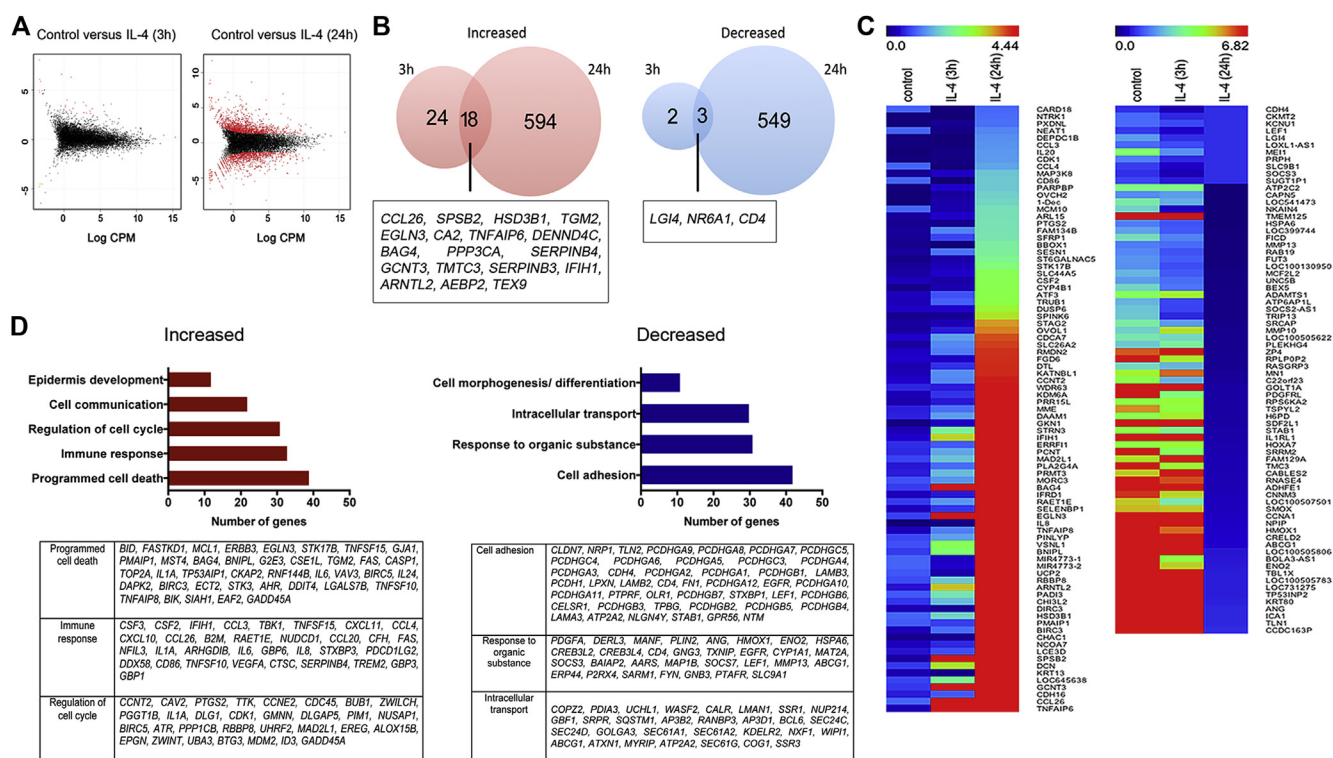


**FIG 1.** IL-4 modifies HK gene expression. HKs were differentiated for 2 days with calcium chloride and stimulated with IL-4 for 3 and 24 hours before RNA-Seq analysis. **A**, Graphic representation of genes that were enriched at least 2-fold in IL-4-stimulated keratinocytes (red dots). **B**, Venn diagram representing the number of genes altered by IL-4 after 3 and 24 hours. **C**, Heat map comparison of gene enrichment in IL-4-stimulated HKs by using MultiExperiment Viewer software. **D**, Gene ontology analysis using the differential expression of genes at 24 hours after IL-4. Clustering was performed by using DAVID Bioinformatics database analysis. Data represent the average of 2 biological replicates for each condition. False discovery rate < 0.1.

## RESULTS

### IL-4 responses in HKs

To begin to define keratinocyte responses to IL-4, we characterized the expression of IL-4 signaling components. Immortalized HKs were cultured for 5 days in calcium chloride and demonstrated increased filaggrin (*FLG*) expression as an indicator of differentiation. Differentiated HKs exhibited greater expression of *STAT6*, *IL4R*, and the inhibitory *IL13RA2* at day 5, contrasting largely unchanged expression of *IL13RA1* during the differentiation period (see Fig E1, A, in this article's Online Repository at [www.jacionline.org](http://www.jacionline.org)). Flow cytometric analysis indicated the percentage of phospho-STAT6 (Tyr641)-positive keratinocytes and the mean fluorescence intensity of phospho-STAT6 peaked 30 minutes after IL-4 stimulation (see Fig E1, B and C). Analysis of gene expression and chemokine production demonstrated decreased expression of the epidermal differentiation complex genes *FLG*, loricrin (*LOR*), and involucrin (*IVL*) after long-term incubation with IL-4 and the induction of *CCL26* expression and secretion after short and long-term incubation with IL-4 (see Fig E1, D-F). The parallels between these responses and those previously published for isolated keratinocytes and skin tissue validated this approach for further study.<sup>8,9,25-27</sup>

To broadly determine IL-4-stimulated transcriptional changes in HKs, we performed RNA-Seq analysis. At day 2 of culture, HKs were incubated in the presence or absence of IL-4 for 3 or 24 hours. After 3 hours, IL-4 stimulation resulted in at least a

2-fold change in the expression of 47 genes when compared with cells cultured with media alone (Fig 1, A and B). After 24 hours, IL-4 stimulation resulted in a differential expression of 1164 genes (Fig 1, A and B). The genes most differentially regulated at both time points are indicated by the heat map in Fig 1, C. Among the transcripts increased at 24 hours that were classified by using DAVID analysis, 39 were associated with regulation of cell death, 33 were involved with immune response and cytokine-receptor interaction, and 31 were involved with cell-cycle regulation (Fig 1, D). Transcripts for proteins involved with cell adhesion, response to organic substances, and intracellular transport and secretion were the largest functional categories of genes with expression decreased by IL-4.

Three-dimensional cultures (human skin equivalents) were treated with IL-4 for 24 hours before testing the expression of 7 IL-4-induced genes to extend these findings. Treatment with IL-4 resulted in a significant increase in *CCL26*, *CA2*, *CISH*, and *SERPINB4* (see Fig E2, A, in this article's Online Repository at [www.jacionline.org](http://www.jacionline.org)). Additionally, the effects of IL-4 on HK monolayer gene expression increased in a dose-dependent manner (see Fig E2, B). Like IL-4, IL-13 alters gene expression in keratinocytes.<sup>12,14</sup> HKs were differentiated and stimulated with IL-4 or IL-13 for 5 days before analyzing the expression of genes to determine whether IL-4 and IL-13 have similar function in regulating HK gene expression. IL-13 decreased *FLG*, *IVL*, *LOR*, and fibronectin 1 (*FNI*) similarly to IL-4 (see Fig E2, C). IL-13 also

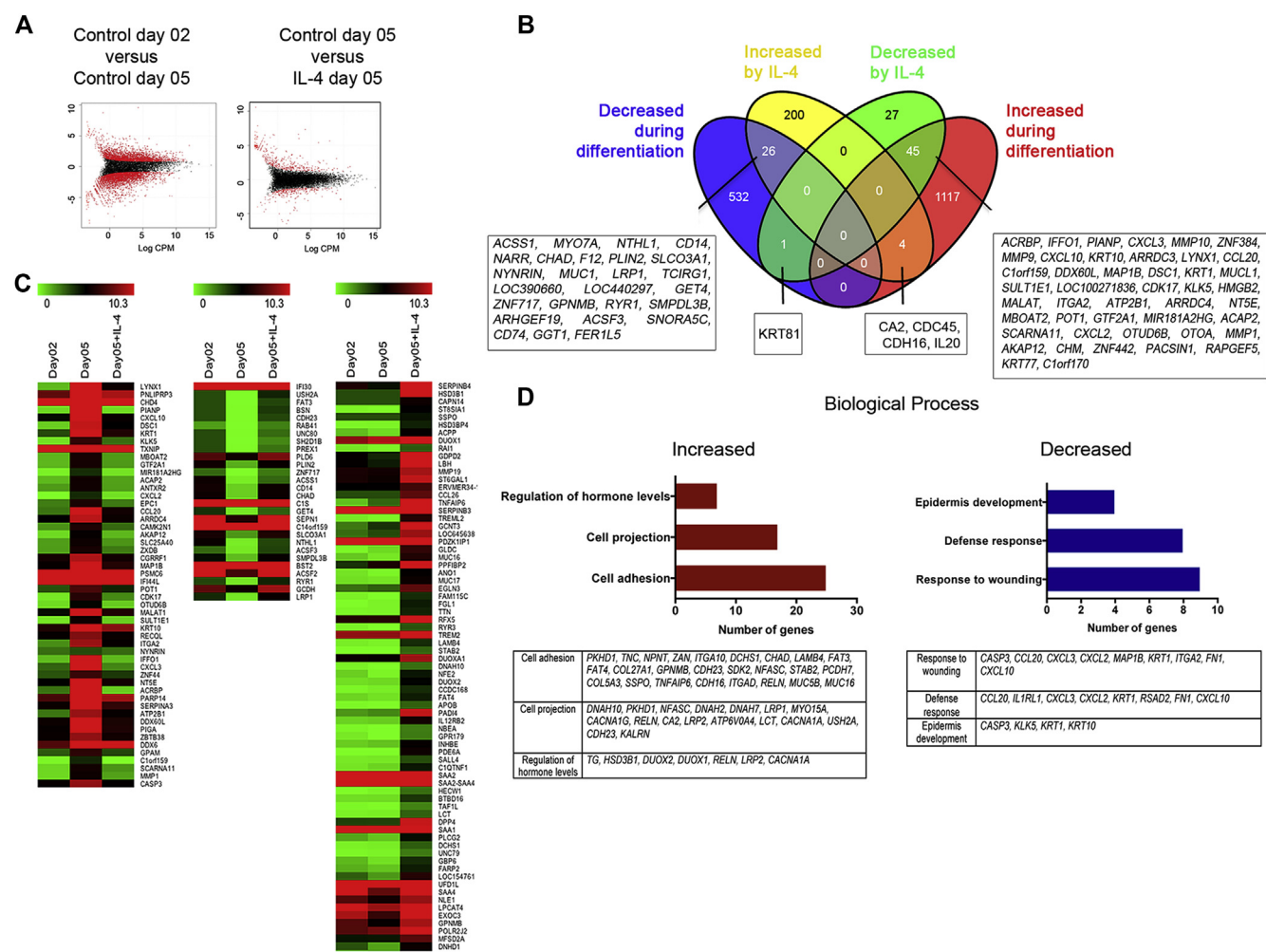


**FIG 2.** Chronic IL-4 stimulation alters gene expression associated with normal differentiation in keratinocytes. HKs were differentiated for 5 days with calcium chloride in the presence or absence of IL-4 before RNA-Seq analysis. **A**, Graphic representation of genes enriched at least 2-fold in control HKs at day 5 of differentiation and in IL-4-stimulated keratinocytes (red dots). **B**, Venn diagram representing the number of genes differentially expressed at day 5 by keratinocytes cultured with calcium chloride alone (compared with day 2) and after IL-4. **C**, Heat map comparison using MultiExperiment Viewer software of gene enrichment in keratinocytes cultured for 2 or 5 days with calcium chloride alone or for 5 days with IL-4. **D**, Gene ontology analysis performed by using genes differentially expressed after 5 days of stimulation with IL-4. Clustering was performed by using DAVID Bioinformatics database analysis. Data represent the average of 2 biological replicates for each condition. False discovery rate < 0.1.

resulted in a comparable increase in *SERPINB3* and *SERPINB4* expression but only a partial increase in *CCL26* and *CISH* expression when compared with IL-4. Collectively, these data showed that acute stimulation of keratinocytes with IL-4 alters the expression of genes encoding proteins with diverse functions that could ultimately influence local inflammatory responses, alter cell proliferation and survival, and favor loss of cell adhesion.

### RNA-Seq analysis of keratinocytes chronically stimulated with IL-4

As shown in Fig E1, D, exposure of keratinocytes to calcium chloride for 5 days resulted in altered expression of differentiation-related genes. Thus to determine whether IL-4 modifies genes expressed by keratinocytes in later phases of differentiation, we performed RNA-Seq analysis of HKs

differentiated for 5 days and incubated with or without IL-4 before comparing the results with HKs cultured for 2 days. HKs differentiated for 5 days exhibited differential expression of 1724 genes when compared with HKs at day 2, with IL-4 altering expression of 303 genes (Fig 2, A and B). The expression pattern for a subset of genes in IL-4-stimulated HKs at day 5 of culture was similar to the expression pattern in control HKs at day 2 (Fig 2, C). IL-4 also increased the expression of a set of genes compared with unstimulated HKs at either time point (Fig 2, C). A Venn diagram shows the 1166 genes increased and 558 genes decreased during HK differentiation (Fig 2, B). IL-4 attenuated differentiation-induced changes in gene expression of 71 genes (45 were decreased and 26 were increased; Fig 2, B). Moreover, IL-4 further augmented the expression of 4 genes and decreased the expression of 1 gene in calcium-differentiated HKs (Fig 2, B). We also observed that IL-4 increased expression

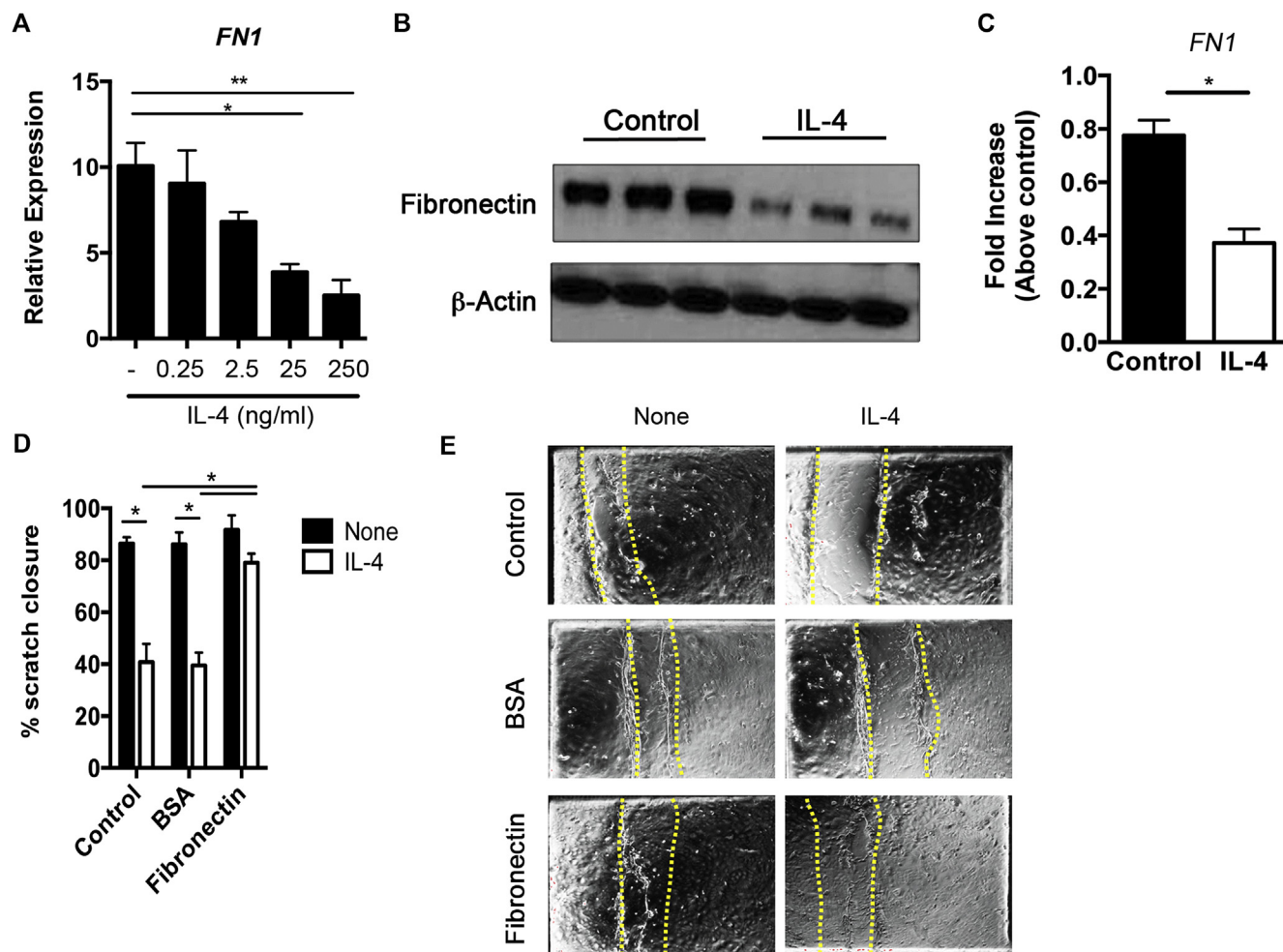


**FIG 3.** IL-4-stimulated keratinocytes show delayed wound healing. **A**, HKs were differentiated for 5 days with calcium chloride in the presence or absence of IL-4 before analysis of *FN1* expression by using quantitative RT-PCR. **B**, Cell lysates were collected, and the expression of fibronectin and  $\beta$ -actin was determined by means of Western blotting. **C**, Gene expression was analyzed 3 hours after scratching by using quantitative RT-PCR. **D**, Percentage of scratches closed after 24 hours of culture. **E**, Microscopy of HKs differentiated with calcium chloride alone or calcium chloride plus IL-4 for 5 days in controls or plates covered with a substratum of BSA or fibronectin. Dashed red lines represent original wounds. Pictures are representative of 4 fields analyzed over at least 3 independent experiments. Data represent the mean of 3 independent experiments. \* $P < .05$  and \*\* $P < .01$ .

of 200 genes and decreased expression of 27 genes in HKs that were not differentially expressed during differentiation (Fig 2, B). A gene ontology analysis of IL-4-regulated genes showed that chronic exposure to IL-4 increased transcription of 25 genes involved with cell adhesion and 17 genes related to cell projection. IL-4 decreased transcription of 9 genes involved with wound healing and 8 genes involved in host defense (Fig 2, D).

### IL-4 impairs the keratinocyte wound-healing response

As noted above, a subset of genes regulated by IL-4 affects the wound repair process. This observation is consistent with diminished wound repair in children who show signs of increased atopy<sup>28</sup> and with the diminished recovery of transepidermal water loss after injury in Stat6VT transgenic mice, a model of allergic skin inflammation.<sup>9,27</sup> To investigate whether IL-4-induced changes in the wound-healing subset of genes alter functional

activity of HKs, we assayed for wound-healing capacity in culture. HKs were differentiated for 2 or 5 days and cultured in the presence or absence of IL-4. Scratches were made in the confluent monolayer to simulate wounding, and wound closure was monitored over 48 hours. Time-lapse analysis showed that differentiated keratinocytes migrate toward the wound area within 24 hours and partially close the wound space (see Fig E3, A, in this article's Online Repository at [www.jacionline.org](http://www.jacionline.org)). Proliferative cells were observed in the area adjacent to the wound edge (see Video E1 in this article's Online Repository at [www.jacionline.org](http://www.jacionline.org)), whereas cells at the edge guided the movement of neighboring cells. In contrast, IL-4-stimulated keratinocytes did not migrate toward the wound edge and exhibited significantly less wound closure in both cultures when compared with the control cells (see Fig E3, B).

Because IL-4 decreases the potential wound-healing response of HKs at days 2 and 5 of differentiation, we used RNA-Seq analysis to better define a target gene involved in reduced

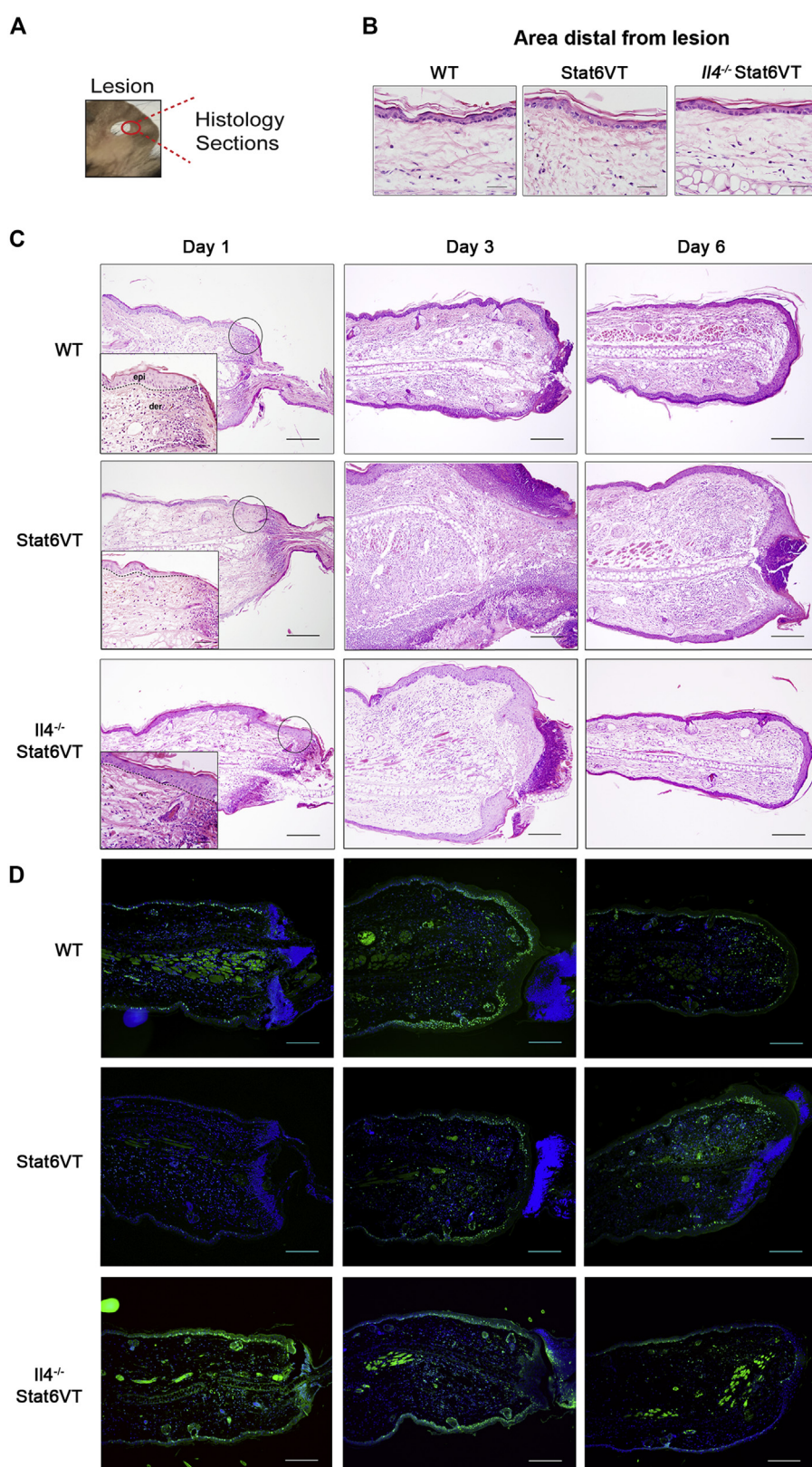


**FIG 4.** Stat6VT mice exhibit delayed wound healing. Lesions were monitored by using hematoxylin and eosin in ears of WT, Stat6VT, and  $\text{II4}^{-/-}$  Stat6VT mice at days 1, 3, and 6 after wounding (dermis [*der*] and epidermis [*epi*] separated by dashed lines). **A**, Representation of ear punch. **B** and **C**, Visualization of histologic sections from distal areas from lesion (Fig 4, B) and lesion re-epithelialization and wound closure (Fig 4, C). **D**, Immunofluorescence for the proliferation marker Ki-67 (green fluorescence) in the ears of WT, STAT6VT, and  $\text{II4}^{-/-}$  Stat6VT mice on indicated days after punch. Nuclei are stained with 4'-6-diamidino-2-phenylindole dihydrochloride in blue. Scale bar = 200  $\mu\text{m}$ . Pictures are representative of 3 to 4 mice from 2 independent experiments.

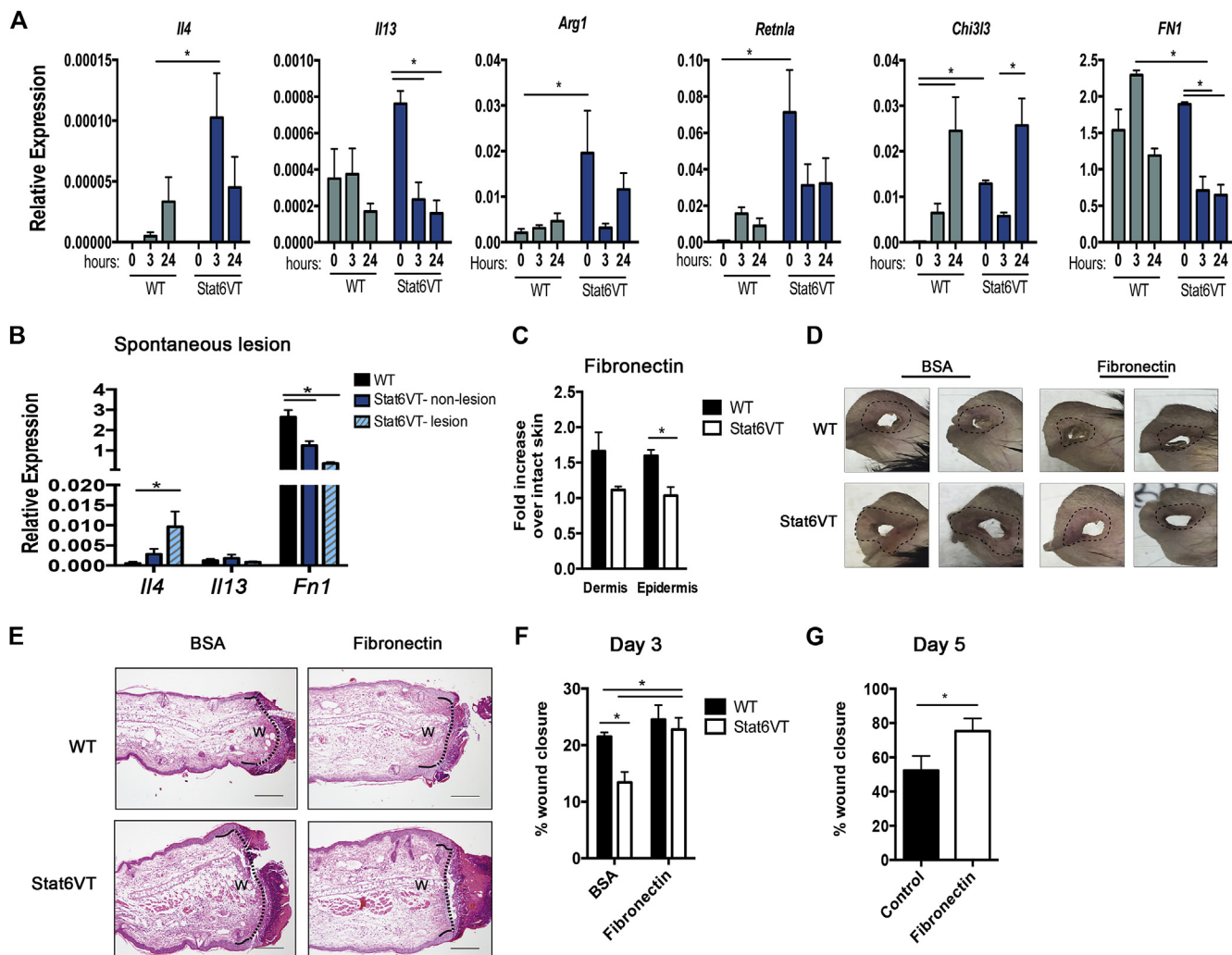


**FIG 5.** Topical fibronectin improves wound-healing potential in Stat6VT mice. **A** and **B**, Gene expression was determined by using quantitative RT-PCR in ears of WT and Stat6VT mice before (0 hour) and 3 and 24 hours after wounding (Fig 5, A) or in nonlesional skin in WT and Stat6VT mice and mice with spontaneous lesions (Fig 5, B). **C**, Fibronectin levels were measured by using ELISA in dermis and epidermis in WT and Stat6VT mice 24 hours after wounding punch. Fold change was determined over intact skin (0 hours). **D** and **E**, Ear representation (Fig 5, D) and lesions monitored by using hematoxylin and eosin staining in ears of WT and Stat6VT at day 3 after wounding (Fig 5, E; open wound size [w] measured by means of morphometry are indicated by dotted black lines). **F** and **G**, Morphometric analysis of percentage of wound closure at day 3 after punch in WT and Stat6VT mice treated with ointment containing BSA or fibronectin (Fig 5, F) or at day 5 after wounding in Stat6VT mice treated with ointment alone or ointment containing fibronectin (Fig 5, G). Data represent means of 2 independent experiments. \* $P < .05$ . Scale bar = 200  $\mu$ m. Pictures are representative of 3 mice from 2 independent experiments.

wounding at both time points. Thus, as we observed, at days 2 and 5 of differentiation, IL-4-treated HKs exhibited reduced *FN1* expression (see Fig E3, C). Keratinocytes cultured with increasing concentrations of IL-4 exhibited reduced levels of *FN1* mRNA (Fig 3, A). These cells also exhibited reduced fibronectin production (Fig 3, B) and decreased *FN1* mRNA expression 3 hours after scratching of monolayers in the *in vitro* wound-healing assay (Fig 3, C).

To further assess whether fibronectin potentiates wound-healing response in IL-4-treated HKs, cells were differentiated for 5 days in control plates, BSA-coated plates, or fibronectin-coated plates and cultured in the presence or absence of IL-4. A quantitative analysis showed that IL-4-treated HKs cultured on a fibronectin substratum exhibited a significant increase in wound

closure when compared with HKs cultured on control or BSA substratum with IL-4 (Fig 3, D and E). Collectively, IL-4 potently inhibits the wound-healing capacity of keratinocytes by inhibiting fibronectin production.

### Impaired skin wound-healing response in models of AD-like disease

Because IL-4 decreased keratinocyte wound closure, mice with spontaneous development of AD-like lesions (Stat6VT mice) were used to test the influence of the allergic environment on *in vivo* wound healing. Stat6VT mice overexpress an active form of STAT6 in T cells, resulting in predominant T<sub>H</sub>2-type cytokine production and allergic skin inflammation.<sup>17,27</sup> Importantly for these studies, Stat6VT expression was observed in CD45<sup>+</sup> cells but

not CD45<sup>-</sup> cells isolated from the dermis and epidermis of transgenic mice and was predominantly observed in CD4<sup>+</sup> cells (see Fig E4 in this article's Online Repository at [www.jacionline.org](http://www.jacionline.org)).

To investigate the re-epithelialization process in an atopic environment, we used an ear punch (2 mm in diameter) to wound ears of 4- to 6-month-old WT, Stat6VT, and *Il4*<sup>-/-</sup> Stat6VT mice (Fig 4, A). It is important to note that there is no difference in the appearance of skin before wounding (Fig 4, B). Through histologic analysis over 6 days after wounding, we monitored lesion re-epithelialization and wound closure. At day 1 after wounding, wounds in all groups of mice exhibited a neutrophilic infiltrate (Fig 4, C). At this time point, only WT and *Il4*<sup>-/-</sup> Stat6VT mice showed a denser epidermis at the wound border (Fig 4, C). Further analysis in the control group (ie, at days 3 and 6) showed a reduction in cellular infiltration and continuous re-epithelialization. In contrast, Stat6VT mice exhibited pronounced tissue inflammation associated with edema and delayed wound closure (Fig 4, C).

Ear sections were stained by means of immunofluorescence with the Ki-67 nuclear protein expressed during cell proliferation to determine whether differences in wound healing in WT, Stat6VT, and *Il4*<sup>-/-</sup> Stat6VT mice correlate with poor epithelial proliferation (Fig 4, D). At all time points, all mice exhibited Ki-67<sup>+</sup> cells in the dermis and epidermis. However, WT and *Il4*<sup>-/-</sup> Stat6VT mice showed more intense staining in the epidermis mainly at days 1 and 3 after skin punch when compared with Stat6VT mice. At day 3, proliferative cells circumscribed most of the lesion in WT mice, and at day 6, the intensity of Ki-67 stain was attenuated. Stat6VT mice exhibited delayed epidermal proliferation and inefficient lesion closure.

WT and *Stat6*<sup>-/-</sup> mice were treated with the vitamin D analog (MC903) for 5 days before wounding to verify whether deficient re-epithelialization also occurs in an induced model of AD-like disease and to determine whether IL-4 signaling normally regulates this process. Wound healing was monitored at days 3 and 6 after punch, and wound closure was measured by using morphometric analysis. We observed a significant decrease in wound closure at day 3 in MC903-treated WT mice compared with that seen in control mice treated with ethanol alone (see Fig E5, A and B, in this article's Online Repository at [www.jacionline.org](http://www.jacionline.org)). Moreover, *Stat6*<sup>-/-</sup> mice exhibited earlier re-epithelialization when compared with WT mice treated with MC903 (see Fig E5, A and B). Thus in models of induced and spontaneous AD, an atopic environment worsens re-epithelialization and wound-healing responses in the skin.

## Topical fibronectin enhances skin wound healing in Stat6VT mice

T<sub>H</sub>2-type cytokines can promote profibrotic pathways involved in tissue regeneration through induction of alternatively activated (M2) macrophage differentiation.<sup>29</sup> However, in our model the IL-4/STAT6 axis decreases skin wound healing. To explore this apparent contradiction, we tested the expression of cytokines and M2 markers in WT and Stat6VT intact ears (0 hour) and 3 and 24 hours after wounding. We observe that *Arg1* (arginase) *Retnla* (*Fizz1*), and *Chi3l3* (*Ym1*) mRNA levels were significantly increased at 0 hours in Stat6VT mice (Fig 5, A) when compared with WT mice. Expression of *Il4*, *Arg1*, and *Retnla* was increased at 3 and 24 hours after wounding in WT mice but did not reach the levels observed in transgenic mice. Additionally, we observed that *Fnl* mRNA expression was similar at 0 hours in

WT and Stat6VT mice (Fig 5, A). However, at 3 hours after wounding, tissue from WT mice showed an increase in fibronectin expression and tissue from Stat6VT mice exhibited a significant reduction in *Fnl* mRNA expression when compared with that in intact ears or WT mice (Fig 5, A). Likewise, *Il4* mRNA levels are increased and *Fnl* mRNA levels are decreased in nonlesional and lesional skin from Stat6VT mice compared with levels seen in intact skin from WT mice (Fig 5, B). Additionally, fibronectin levels measured by means of ELISA were significantly lower in the epidermis of Stat6VT mice at 24 hours after wounding when compared with samples from WT mice (Fig 5, C).

Because fibronectin production was reduced in HK cultures after IL-4 stimulation and because this protein increased IL-4-stimulated HK scratch closure, we next determined whether topical application of fibronectin accelerates wound healing in allergic mice. WT and Stat6VT mice were treated with ointment containing 10 µg of BSA or fibronectin right after (day 1) and 24 hours after (day 2) wounding to test the involvement of fibronectin in the Stat6VT mouse wound-healing response. Histologic analyses were performed at day 3, a period when partial re-epithelialization was observed (Fig 4, C). Macroscopic analysis revealed fibronectin treatment improved tissue recovery and erythema surrounding the lesion (Fig 5, D). In histologic analysis (Fig 5, E) and morphometric analysis (Fig 5, F) topical fibronectin treatment significantly improved wound closure in Stat6VT mice compared with that seen in control protein-treated mice but had modest effects on WT mice. We also observed that fibronectin significantly increased wound closure in Stat6VT mice at day 5 after wounding when compared with that seen in Stat6VT mice receiving ointment alone as control (Fig 5, G). Thus although IL-4 affects the expression of various genes directly involved in response to wounding, the IL-4-dependent repression in fibronectin expression appears to be a major target in contributing to the reduction of wound-healing potential of keratinocytes in an allergic environment.

## DISCUSSION

IL-4 promotes the development of atopic diseases through effects on multiple cell types. Despite its critical role in AD, how IL-4 alters gene expression in keratinocytes has not been completely defined. In this report we use high-throughput transcriptomic analysis to identify IL-4-induced changes in keratinocyte gene expression at early and late stages of differentiation. Acute and chronic IL-4 stimulation resulted in extensive changes in gene expression profiles that spanned a variety of functional modules, including wound healing, a biological response impaired by IL-4. Moreover, central for IL-4-mediated effects in delayed wound healing was reduction in fibronectin production.

IL-4 alters a number of biological processes in keratinocytes, and cells in different stages of differentiation showed changes in distinct functions. Acute IL-4 stimulation (3 and 24 hours) resulted in alterations in genes involved in cell growth and survival and diminished expression of genes involved in cell adhesion, which together might contribute to epidermal hyperplasia, spongiosis, and diminished barrier function, all characteristics of lesional skin of patients with AD.<sup>30-32</sup> At day 5 of differentiation, IL-4 increased expression of genes involved in cell projection and adhesion and decreased expression of genes participating in response to wounding and defense. In fact, a subset of genes in IL-4-stimulated differentiated HKs (day 5) was

similar in expression to less differentiated HKs (day 2). These changes might favor a less organized epithelial structure and contribute to an increased susceptibility to infection, which are also characteristics of AD lesions.<sup>33,34</sup> Although most of the experiments used immortalized HKs and these might not entirely replicate intact skin, similar responses were observed with primary keratinocytes and skin equivalents made with primary cells. Moreover, several genes induced by IL-4, including *CCL26*, *S100A7*, *S100A12*, *IL12RB*, *LCE3E*, *SERPINB3*, *SERPINB4*, and *ADAMTS4*, were also increased in skin from patients with AD,<sup>35,36</sup> indicating a possible role for IL-4 in mediating many skin barrier abnormalities in patients with AD.

Intense pruritis is a characteristic and often debilitating feature of AD, causing patients to scratch and consequently wound their skin.<sup>37</sup> Lesions are frequently associated with areas that patients readily reach to scratch.<sup>38,39</sup> As our data indicate, IL-4 exposure might also contribute to AD pathogenesis by impairing appropriate wound repair. Using scratching of keratinocyte monolayers and time-lapse video microscopy, we demonstrate a significant decrease in recovery of the monolayer after IL-4 exposure. This observation could be linked to reports that children with AD demonstrating greater atopic responses had increased healing time of lesions.<sup>28</sup> In contrast to the wound-healing process observed here, recovery of barrier function after tape stripping of nonlesional skin in patients with AD and healthy control subjects was similar.<sup>40</sup> de Koning et al<sup>41</sup> reported no differences in gene expression between tape-striped nonlesional skin of patients with AD versus skin from healthy control subjects, suggesting that decreased wound healing would most likely be observed in skin with a wound more severe than superficial tape stripping or in skin with an active inflammatory response.

IL-4 has been shown previously to be a prohealing cytokine in wound repair.<sup>29,42-45</sup> Our studies differ from these studies in several ways. First, we are focusing on re-epithelialization of the skin, rather than fibrosis and repair below the keratinocyte layers. We observed diminished re-epithelialization in 2 models of AD-like skin inflammation, and impaired healing was not observed when mice had defects in IL-4 signaling, suggesting this is a consistent effect of a proatopic environment. Importantly, we did not observe any defects in collagen deposition in the dermis during healing (data not shown).

Second, the IL-4 induced during wound repair in WT mice is much less than observed in atopic models. We directly demonstrated that M2 gene expression, a common target of IL-4 in wound-healing studies, is already greater before wounding in skin from "atopic" mice. Moreover, induction of these genes is increased in the skin of atopic mice. Together, these observations support a model wherein a low level of IL-4, functioning particularly in the dermis, is important for a healing response. However, in an atopic environment IL-4 is at sufficiently high concentrations to alter keratinocyte function and dermal M2 gene expression. In this respect it is not clear that the effects of IL-4 on fibronectin production are strictly on keratinocytes. In our analyses we observed diminished fibronectin protein levels in both the dermis and epidermis, suggesting that other cells might be affected by IL-4 in a similar fashion. Still, the *in vivo* results are consistent with the *in vitro* keratinocyte cultures, demonstrating an important contribution of keratinocyte-produced fibronectin in re-epithelialization.

It is difficult to separate the direct effects of IL-4 in these models versus the effect of IL-4-dependent inflammation in AD

models. We observed that there was greater loss of fibronectin expression in lesional than nonlesional skin of Stat6VT mice. However, there was also greater *Il4* expression in lesional skin, demonstrating that these factors are linked. Although the *in vivo* phenotype is consistent with the *in vitro* observations of keratinocyte function, we cannot exclude a contribution of additional cell types *in vivo* that are responding to IL-4 and mediating some of the delayed healing through secondary effects.

Although IL-4 modifies many genes involved in the wound response,<sup>42</sup> decreased fibronectin expression directly contributed to the *in vitro* impairment of HK monolayer wound closure. Fibronectin is a multidomain protein component of the extracellular matrix that is expressed in high levels at wound sites.<sup>46,47</sup> It is associated with wound repair through, among other mechanisms during injury, enhancing growth factor binding stability and cell survival.<sup>48,49</sup> Although topical application of fibronectin in lesions of Stat6VT mice only partially restored re-epithelialization, this protein significantly improved the appearance of lesions, including decreasing erythema in the tissue. Many functions regulated by fibronectin, including adhesion, migration, and differentiation,<sup>50</sup> were also functions affected in HKs after IL-4 stimulation. Thus whether fibronectin can be used to treat AD lesions or other biological defects induced by IL-4 in keratinocytes is an interesting question remaining to be investigated.

Together, our findings describe a comprehensive role for IL-4 in preventing keratinocyte maturation by influencing the expression of key genes affecting skin barrier function. Induction of a subset of genes by IL-4 was confirmed in skin equivalents, and a deficient response of keratinocytes from allergic mice to wounding was also observed *in vivo*, further supporting a physiologic role for these studies. The more detailed understanding of IL-4-regulated genetic programs in keratinocytes described in this report should lead to additional insights into the development of allergic skin disease.

We thank Yunlong Liu for guidance in bioinformatics analyses. We also thank Drs Janice Blum, Matthew Olson, Matthew Hufford, and Jeffrey Travers for review of this manuscript. Finally, we thank David H. Southern for assistance with cell culture.

### Key messages

- IL-4, a critical effector cytokine in patients with AD, repressed expression of genes induced during keratinocyte differentiation.
- Keratinocytes exposed to IL-4 have changes in expression of more than 1000 genes.
- IL-4 impaired the wound-healing response of keratinocytes by decreasing fibronectin production.
- Topical fibronectin increases wound healing in mice with spontaneous AD-like disease.

### REFERENCES

1. Leung DY, Boguniewicz M, Howell MD, Nomura I, Hamid QA. New insights into atopic dermatitis. *J Clin Invest* 2004;113:651-7.
2. Sehra S, Tuana FM, Holbreich M, Mousdicas N, Tepper RS, Chang CH, et al. Scratching the surface: towards understanding the pathogenesis of atopic dermatitis. *Crit Rev Immunol* 2008;28:15-43.

3. Albanesi C, Fairchild HR, Madonna S, Scarponi C, De Pita O, Leung DY, et al. IL-4 and IL-13 negatively regulate TNF-alpha- and IFN-gamma-induced beta-defensin expression through STAT-6, suppressor of cytokine signaling (SOCS)-1, and SOCS-3. *J Immunol* 2007;179:984-92.
4. Beltraní VS. Suggestions regarding a more appropriate understanding of atopic dermatitis. *Curr Opin Allergy Clin Immunol* 2005;5:413-8.
5. Bergmann RL, Edenharder G, Bergmann KE, Forster J, Bauer CP, Wahn V, et al. Atopic dermatitis in early infancy predicts allergic airway disease at 5 years. *Clin Exp Allergy* 1998;28:965-70.
6. Gustafsson D, Sjoberg O, Foucard T. Development of allergies and asthma in infants and young children with atopic dermatitis—a prospective follow-up to 7 years of age. *Allergy* 2000;55:240-5.
7. Howell MD, Gallo RL, Boguniewicz M, Jones JF, Wong C, Streib JE, et al. Cytokine milieu of atopic dermatitis skin subverts the innate immune response to vaccinia virus. *Immunity* 2006;24:341-8.
8. Rouse BT, Sehrawat S. Immunity and immunopathology to viruses: what decides the outcome? *Nat Rev Immunol* 2010;10:514-26.
9. Kim BE, Leung DY, Boguniewicz M, Howell MD. Loricrin and involucrin expression is down-regulated by Th2 cytokines through STAT-6. *Clin Immunol* 2008;126:332-7.
10. Wills-Karp M, Finkelman FD. Untangling the complex web of IL-4- and IL-13-mediated signaling pathways. *Sci Signal* 2008;1:pe55.
11. Nelms K, Keegan AD, Zamorano J, Ryan JJ, Paul WE. The IL-4 receptor: signaling mechanisms and biological functions. *Annu Rev Immunol* 1999;17:701-38.
12. Kagami S, Saeki H, Komine M, Kakinuma T, Tsunemi Y, Nakamura K, et al. Interleukin-4 and interleukin-13 enhance CCL26 production in a human keratinocyte cell line, HaCaT cells. *Clin Exp Immunol* 2005;141:459-66.
13. Pellerin L, Henry J, Hsu CY, Balica S, Jean-Decoster C, Mechlin MC, et al. Defects of filaggrin-like proteins in both lesional and nonlesional atopic skin. *J Allergy Clin Immunol* 2013;131:1094-102.
14. Omori-Miyake M, Yamashita M, Tsunemi Y, Kawashima M, Yagi J. In vitro assessment of IL-4- or IL-13-mediated changes in the structural components of keratinocytes in mice and humans. *J Invest Dermatol* 2014;134:1342-50.
15. Owczarek W, Paplinska M, Targowski T, Jahnz-Roziky K, Paluchowska E, Kucharczyk A, et al. Analysis of eotaxin 1/CCL11, eotaxin 2/CCL24 and eotaxin 3/CCL26 expression in lesional and non-lesional skin of patients with atopic dermatitis. *Cytokine* 2010;50:181-5.
16. Lewkowich IP, Lajoie S, Clark JR, Herman NS, Sproles AA, Wills-Karp M. Allergen uptake, activation, and IL-23 production by pulmonary myeloid DCs drives airway hyperresponsiveness in asthma-susceptible mice. *PLoS One* 2008;3:e3879.
17. Bruns HA, Schindler U, Kaplan MH. Expression of a constitutively active Stat6 in vivo alters lymphocyte homeostasis with distinct effects in T and B cells. *J Immunol* 2003;170:3478-87.
18. Kaplan MH, Schindler U, Smiley ST, Grusby MJ. Stat6 is required for mediating responses to IL-4 and for development of Th2 cells. *Immunity* 1996;4:313-9.
19. Wang Q, Du J, Zhu J, Yang X, Zhou B. Thymic stromal lymphopoietin signaling in CD4(+) T cells is required for TH2 memory. *J Allergy Clin Immunol* 2015;135:781-91.e3.
20. Kuhn C, Hurwitz SA, Kumar MG, Cotton J, Spandau DF. Activation of the insulin-like growth factor-1 receptor promotes the survival of human keratinocytes following ultraviolet B irradiation. *Int J Cancer* 1999;80:431-8.
21. Dickson MA, Hahn WC, Ino Y, Ronfard V, Wu JY, Weinberg RA, et al. Human keratinocytes that express hTERT and also bypass a p16(INK4a)-enforced mechanism that limits life span become immortal yet retain normal growth and differentiation characteristics. *Mol Cell Biol* 2000;20:1436-47.
22. Sehrawat S, Reddy PB, Rajasagi N, Suryawanshi A, Hirashima M, Rouse BT. Galectin-9/TIM-3 interaction regulates virus-specific primary and memory CD8 T cell response. *PLoS Pathog* 2010;6:e1000882.
23. Sehrawat S. The omission of comprehensive care: an analysis of the Nursing Home Reform Act of 1987. *J Gerontol Soc Work* 2010;53:64-76.
24. Huang da W, Sherman BT, Lempicki RA. Bioinformatics enrichment tools: paths toward the comprehensive functional analysis of large gene lists. *Nucleic Acids Res* 2009;37:1-13.
25. Lim EJ, Lu TX, Blanchard C, Rothenberg ME. Epigenetic regulation of the IL-13-induced human eotaxin-3 gene by CREB-binding protein-mediated histone 3 acetylation. *J Biol Chem* 2011;286:13193-204.
26. Krishnamurthy P, Sherrill JD, Parashette K, Goenka S, Rothenberg ME, Gupta S, et al. Correlation of increased PARP14 and CCL26 expression in biopsies from children with eosinophilic esophagitis. *J Allergy Clin Immunol* 2014;133:577-80.
27. Sehra S, Yao Y, Howell MD, Nguyen ET, Kansas GS, Leung DY, et al. IL-4 regulates skin homeostasis and the predisposition toward allergic skin inflammation. *J Immunol* 2010;184:3186-90.
28. Ricci G, Patrizi A, Baldi E, Menna G, Tabanelli M, Masi M. Long-term follow-up of atopic dermatitis: retrospective analysis of related risk factors and association with concomitant allergic diseases. *J Am Acad Dermatol* 2006;55:765-71.
29. Knipper JA, Willenborg S, Brinckmann J, Bloch W, Maass T, Wagener R, et al. Interleukin-4 receptor alpha signaling in myeloid cells controls collagen fibril assembly in skin repair. *Immunity* 2015;43:803-16.
30. De Benedetto A, Rafaelis NM, McGirt LY, Ivanov AI, Georas SN, Cheadle C, et al. Tight junction defects in patients with atopic dermatitis. *J Allergy Clin Immunol* 2011;127:773-86, e1-7.
31. De Benedetto A, Slifka MK, Rafaelis NM, Kuo IH, Georas SN, Boguniewicz M, et al. Reductions in claudin-1 may enhance susceptibility to herpes simplex virus 1 infections in atopic dermatitis. *J Allergy Clin Immunol* 2011;128:242-6.e5.
32. Malaisse J, Bourguignon V, De Vuyst E, Lambert de Rouvroit C, Nikkels AF, Flaman B, et al. Hyaluronan metabolism in human keratinocytes and atopic dermatitis skin is driven by a balance of hyaluronan synthases 1 and 3. *J Invest Dermatol* 2014;134:2174-82.
33. Leung DY, Gao PS, Grigoryev DN, Rafaelis NM, Streib JE, Howell MD, et al. Human atopic dermatitis complicated by eczema herpeticum is associated with abnormalities in IFN-gamma response. *J Allergy Clin Immunol* 2011;127:965-73, e1-5.
34. Kobayashi T, Glatz M, Horiuchi K, Kawasaki H, Akiyama H, Kaplan DH, et al. Dysbiosis and *Staphylococcus aureus* colonization drives inflammation in atopic dermatitis. *Immunity* 2015;42:756-66.
35. Renard E, Poree B, Chadjchristos C, Kyriouli M, Maneix L, Bigot N, et al. Sox9/Sox6 and Sp1 are involved in the insulin-like growth factor-I-mediated up-regulation of human type II collagen gene expression in articular chondrocytes. *J Mol Med (Berl)* 2012;90:649-66.
36. Suarez-Farinás M, Tintle SJ, Shemer A, Chiricozzi A, Nogales K, Cardinale I, et al. Nonlesional atopic dermatitis skin is characterized by broad terminal differentiation defects and variable immune abnormalities. *J Allergy Clin Immunol* 2011;127:954-64, e1-4.
37. Elmariah SB, Lerner EA. The missing link between itch and inflammation in atopic dermatitis. *Cell* 2013;155:267-9.
38. Kimura T, Miyazawa H. The ‘butterfly’ sign in patients with atopic dermatitis: evidence for the role of scratching in the development of skin manifestations. *J Am Acad Dermatol* 1989;21:579-80.
39. Amon U, Wolff HH. Healing of chronic atopic dermatitis lesions in skin areas of paraplegia after trauma. *J Dermatol* 1994;21:982-3.
40. Tanaka M, Chen YX, Tagami H. Normal recovery of the stratum corneum barrier function following damage induced by tape stripping in patients with atopic dermatitis. *Br J Dermatol* 1997;136:966-7.
41. de Koning HD, van den Bogaard EH, Bergboer JG, Kamsteeg M, van Vlijmen-Willems IM, Hitomi K, et al. Expression profile of cornified envelope structural proteins and keratinocyte differentiation-regulating proteins during skin barrier repair. *Br J Dermatol* 2012;166:1245-54.
42. Brauweiler AM, Goleva E, Hall CF, Leung DY. Th2 cytokines suppress lipoteichoic acid-induced matrix metalloproteinase expression and keratinocyte migration in response to wounding. *J Invest Dermatol* 2015;135:2550-3.
43. Leoni G, Neumann PA, Sumagin R, Denning TL, Nusrat A. Wound repair: role of immune-epithelial interactions. *Mucosal Immunol* 2015;8:959-68.
44. Allen JE, Wynn TA. Evolution of Th2 immunity: a rapid repair response to tissue destructive pathogens. *PLoS Pathog* 2011;7:e1002003.
45. Wynn TA, Ramalingam TR. Mechanisms of fibrosis: therapeutic translation for fibrotic disease. *Nat Med* 2012;18:1028-40.
46. Brown LF, Dubin D, Lavigne L, Logan B, Dvorak HF, Van de Water L. Macrophages and fibroblasts express embryonic fibronectins during cutaneous wound healing. *Am J Pathol* 1993;142:793-801.
47. Li-Korotky HS, Hebda PA, Lo CY, Dohar JE. Age-dependent differential expression of fibronectin variants in skin and airway mucosal wounds. *Arch Otolaryngol Head Neck Surg* 2007;133:919-24.
48. Zhu J, Clark RA. Fibronectin at select sites binds multiple growth factors and enhances their activity: expansion of the collaborative ECM-GF paradigm. *J Invest Dermatol* 2014;134:895-901.
49. Lin F, Zhu J, Tonnesen MG, Taira BR, McClain SA, Singer AJ, et al. Fibronectin peptides that bind PDGF-BB enhance survival of cells and tissue under stress. *J Invest Dermatol* 2014;134:1119-27.
50. Livant DL, Brabec RK, Kurachi K, Allen DL, Wu Y, Haaseth R, et al. The PHSRN sequence induces extracellular matrix invasion and accelerates wound healing in obese diabetic mice. *J Clin Invest* 2000;105:1537-45.

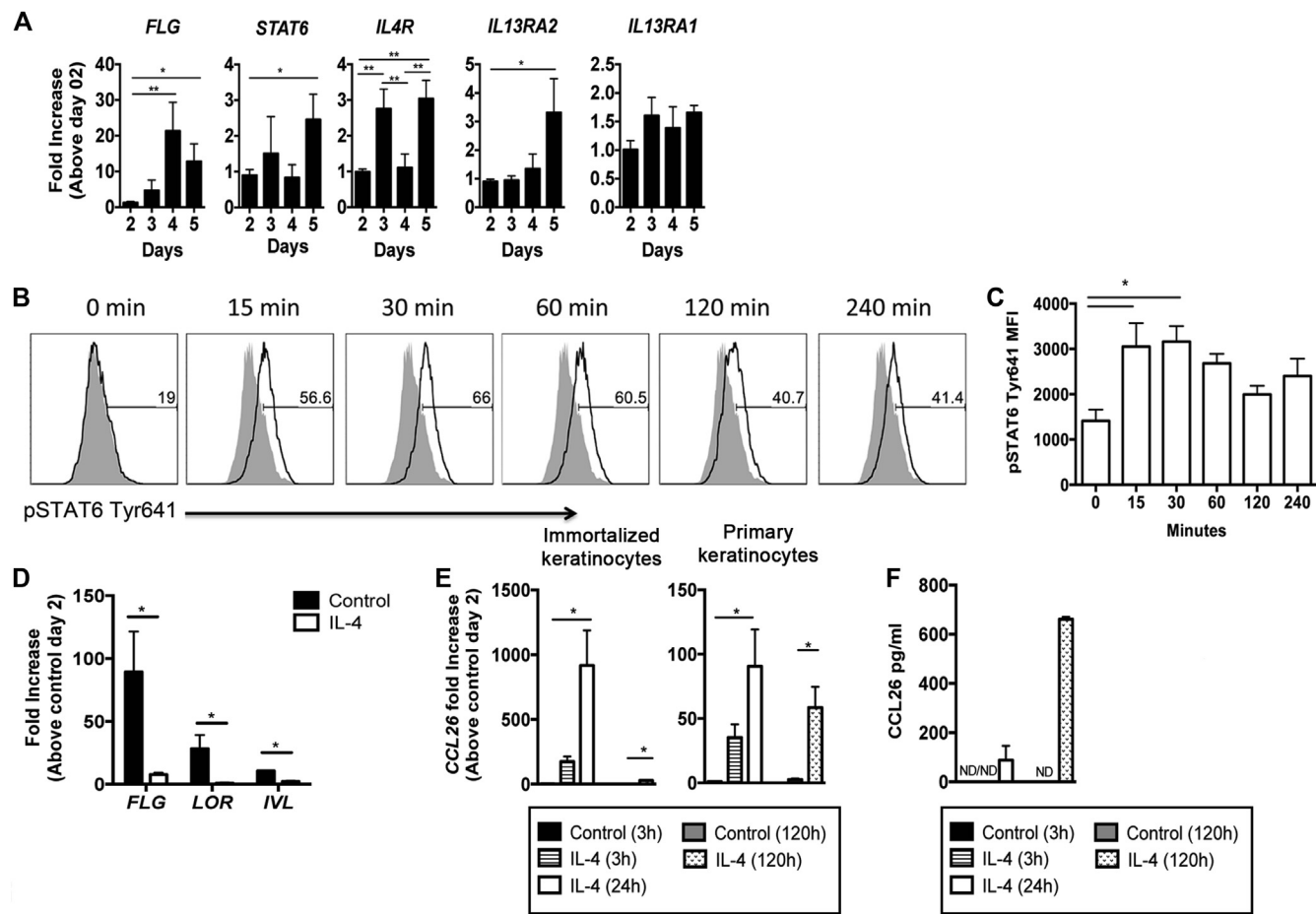


**FIG E1.** IL-4 induces STAT6 activation and CCL26 production by HKs. **A**, HKs were differentiated with calcium chloride, and gene expression was analyzed by using quantitative RT-PCR. **B**, Expression of phospho-STAT6 Tyr641 was determined at the indicated time points after IL-4 stimulation (solid gray line, control; black line, anti-phospho-STAT6 Tyr641). **C**, Phospho-STAT6 mean fluorescence intensity in IL-4-stimulated HKs. **D** and **E**, Gene expression determined by using quantitative RT-PCR in HKs differentiated with calcium chloride and stimulated with IL-4 for 5 days or at the indicated times. **F**, Supernatants from primary keratinocyte culture were assessed for CCL26 production by using ELISA. Data represent mean  $\pm$  SEM of 3 independent experiments. \* $P < .05$  and \*\* $P < .01$ .

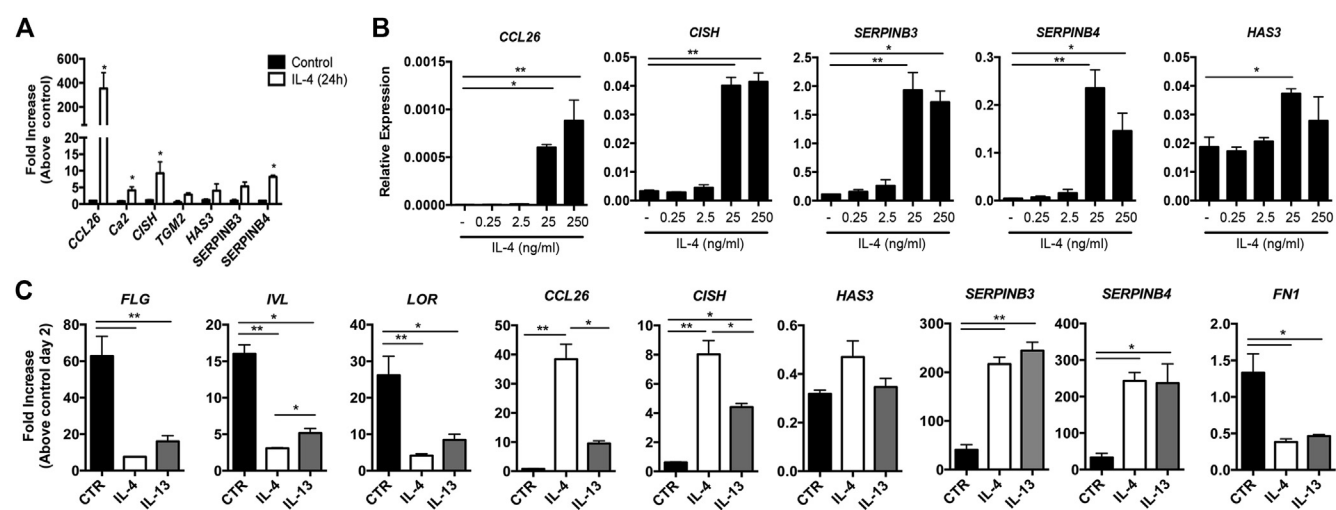


**FIG E2.** Evaluation of IL-4 and IL-13 effects in regulating gene expression by HKs. **A** and **B**, Gene expression was determined by using quantitative RT-PCR in organotypic skin equivalent with IL-4 for 24 hours (Fig E2, A) or in HKs differentiated for 5 days with the indicated concentration of IL-4 (Fig E2, B). **C**, HKs were differentiated with calcium chloride and stimulated with IL-4 or IL-13 for 2 or 5 days before analysis of gene expression. Data represent mean  $\pm$  SEM of 2 independent experiments. \* $P < .05$  and \*\* $P < .01$ .

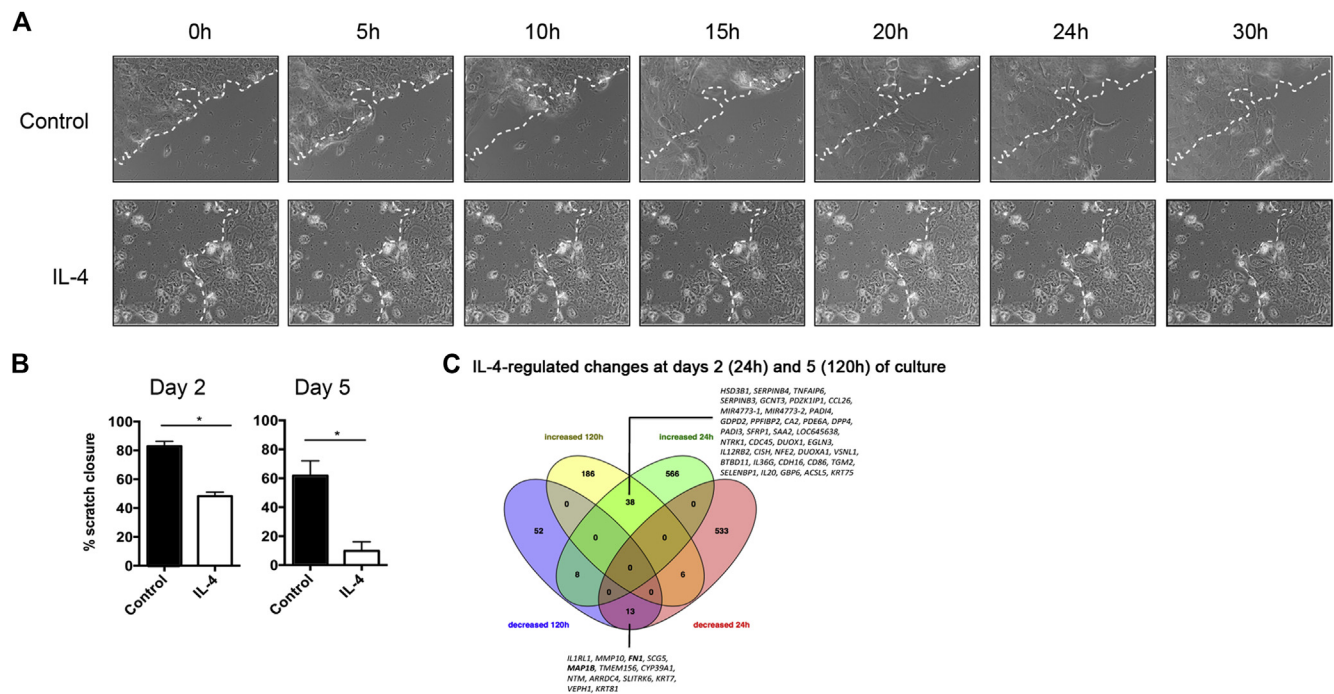


**FIG E3.** IL-4 delays wound healing *in vitro*. **A**, Microscopy of HKs differentiated with calcium chloride alone (Control) or calcium chloride plus IL-4 for 5 days. **B**, Percentage of scratches closed 24 hours after scratching in HKs differentiated for 2 or 5 days with calcium chloride alone or calcium chloride plus IL-4. **C**, Venn diagram representing the number of genes altered by IL-4 after 24 and 120 hours. Pictures are representative of 4 fields analyzed over at least 2 independent experiments. Data represents represent mean  $\pm$  SEM of 2 independent experiments. \* $P$  < .05.

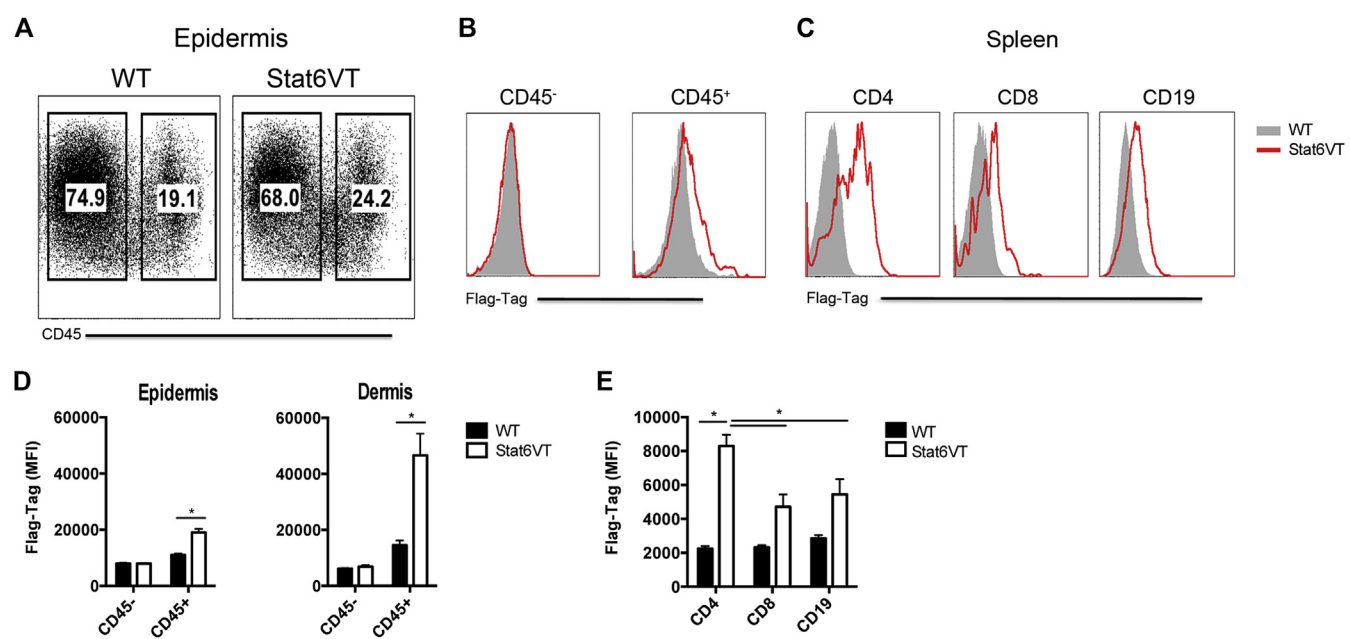


**FIG E4.** Analysis of Stat6VT in different subsets of cells in the skin of mutated mice. **A**, Epidermis was isolated from WT and Stat6VT mice, and CD45<sup>+</sup> and CD45<sup>-</sup> cells were gated as indicated. **B** and **C**, Expression of STAT6VT was analyzed in CD45<sup>+</sup> and CD45<sup>-</sup> cells in the epidermis (Fig E4, **B**) and in CD4<sup>+</sup>, CD8<sup>+</sup>, and CD19<sup>+</sup> cells in spleens (Fig E4, **C**) through FLAG-tag antibody (*solid gray line*, WT mice; *red line*, Stat6VT mice). **D** and **E**, FLAG-tag mean fluorescence intensity in CD45<sup>+</sup> and CD45<sup>-</sup> cells in the epidermis and dermis (Fig E4, **D**) and in lymphocytes in spleens from WT and Stat6VT mice (Fig E4, **E**). Data represent mean  $\pm$  SEM of 2 independent experiments. \* $P < .05$ .

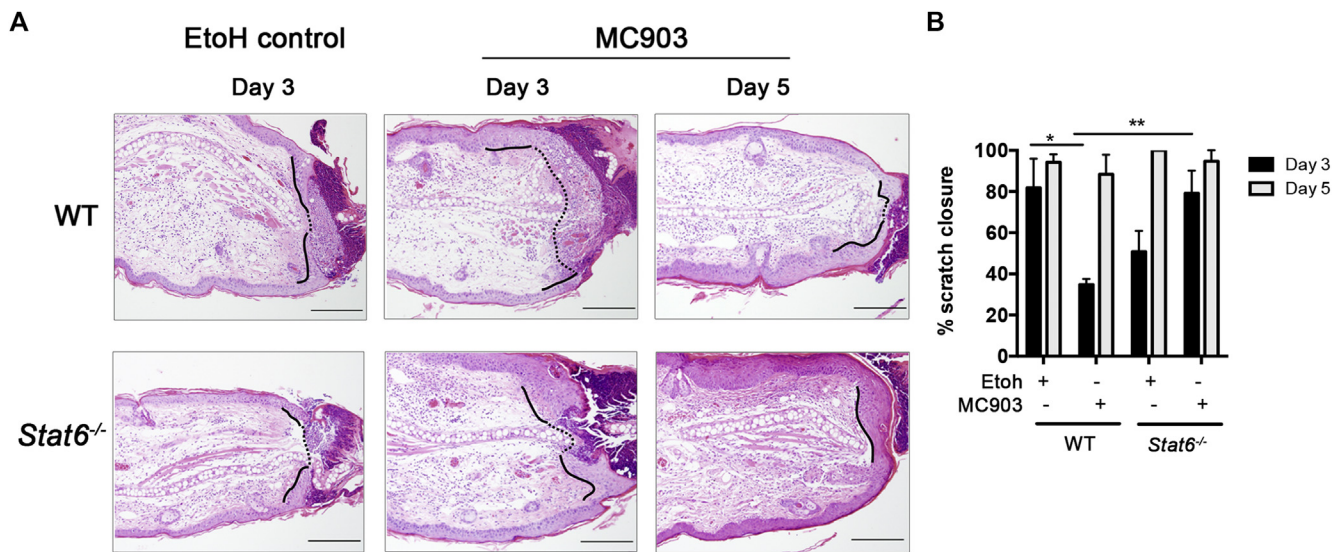


**FIG E5.** Effects of AD-like lesions induced by vitamin D analog on wound healing. Ears of WT and *Stat6*<sup>-/-</sup> mice were treated topically for 5 days with MC903 or ethanol alone. **A**, At day 6, ears were punched, and lesions were monitored by using hematoxylin and eosin at days 3 and 6. **B**, Morphometric analysis of percentage of wound closure. Scale bar = 200  $\mu$ m. Pictures are representative of 3 to 4 mice. \* $P < .05$  and \*\* $P < .01$ .